

# CLUSTER SELECTION AND THE EVOLUTION OF BRIGHTEST CLUSTER GALAXIES

D. J. BURKE<sup>1,2,5</sup>, C. A. COLLINS<sup>1,5</sup>, R. G. MANN<sup>3,4,5</sup>

*Accepted for publication in ApJ Letters*

## ABSTRACT

The K-band Hubble diagram of Brightest Cluster Galaxies (BCGs) is presented for a large, X-ray selected cluster sample extending out to  $z = 0.8$ . The controversy over the degree of BCG evolution is shown to be due to sample selection, since the BCG luminosity depends upon the cluster environment. Selecting only the most X-ray luminous clusters produces a BCG sample which shows, under the assumption of an Einstein-de Sitter cosmology, significantly less mass growth than that predicted by current semi-analytic galaxy formation models, and significant evidence of any growth only if the dominant stellar population of the BCGs formed relatively recently ( $z \leq 2.6$ ).

*Subject headings:* Galaxies: clusters: general — galaxies: elliptical and lenticular, cD — galaxies: evolution — galaxies: formation

## 1. INTRODUCTION

The majority of stars in giant ellipticals found in the cores of rich galaxy clusters are old; photometric and spectroscopic studies of cluster galaxies out to  $z \approx 1$  suggest a formation redshift,  $z_f$ , greater than 2, with little variation within a cluster, and that secondary bursts of star formation account for a small fraction of the stellar mass (e.g. Aragón-Salamanca et al. 1993; Ellis et al. 1997; Stanford, Eisenhardt & Dickinson 1998; van Dokkum et al. 1998; Poggianti et al. 1999).

However, to understand the process of galaxy formation it is necessary to know where the stars were formed as well as when. In the traditional view of early-type galaxy formation—a “monolithic” collapse at high redshift (e.g. Eggen, Lynden-Bell & Sandage 1962; Larson 1969)—all the stars were formed in situ, in direct contrast to the merger-driven growth of galaxies predicted by semi-analytical models for hierarchical cosmologies, such as CDM (e.g. Kauffmann & White 1993; Baugh, Cole & Frenk 1996). Since the ages of the stars are similar in both scenarios, it is the change in mass with look-back time that separates the two pictures observationally. The current data are inconclusive; for example, the hierarchical models are favored by the enhanced merger fraction seen in the  $z = 0.8$  cluster MS1054.4-0321 (van Dokkum et al. 1999), whilst De Propris et al. (1999) show no evidence for mass evolution of bright ellipticals in clusters out to  $z \approx 1$ . In general it is difficult to follow the evolutionary history of ellipticals since selection methods can seriously bias the samples, c.f. the discussions of progenitor bias in van Dokkum & Franx (1996), the effect of preferential selection of the most massive objects at each epoch in Kauffmann & Charlot (1998), and the use of color selection in Jimenez et al. (1999).

One approach to minimising such problems is to study the evolution of a particular class of ellipticals—brightest

cluster galaxies (BCGs)—because of their unique location, close to the center of the cluster’s potential well. BCGs do not appear to be drawn from the same luminosity function as other cluster galaxies (e.g. Dressler 1978), which suggests that they have a distinct formation history. Knowledge of BCG evolution can therefore provide different constraints on galaxy formation models to studies of the general cluster population.

The K-band Hubble diagram for BCGs has recently been extended to  $z \approx 1$  by both Collins & Mann (1998; hereafter CM98) and Aragón-Salamanca, Baugh & Kauffmann (1998; hereafter ABK98): these observations provide the opportunity to measure the luminosity evolution of BCGs since evolutionary and pass-band corrections are insensitive to the recent star-formation history of a galaxy at near-IR wavelengths (e.g. Bershadsky 1995; Madau, Pozzetti, & Dickinson 1998). The conclusions drawn are contradictory, despite the use of the same cosmology and a common assumption that the stellar populations of BCGs are old and passively evolving; CM98 assert that the stellar populations of BCGs in the most massive clusters have not grown significantly since  $z \approx 1$ , whilst ABK98 argue that their results are in good agreement with the mass increase of BCGs—by a factor of four in an Einstein-de Sitter cosmology—predicted by semi-analytical models over the same redshift range. The two samples have almost no overlap—CM98 having used an X-ray selected cluster catalogue whilst ABK98 used a heterogeneous compilation that was mainly optically selected—and it is the aim of the present work to show that the results can be reconciled by considering the properties of the clusters in the two samples. Section 2 describes the BCG sample used—an extension of that of CM98—and the reduction methods employed, whilst section 3 presents the results of the analysis and a comparison to those of ABK98. Throughout this letter an Einstein-de Sitter cos-

<sup>1</sup>Astrophysics Research Institute, Liverpool John Moores University, 12 Quays House, Egerton Wharf, Birkenhead, CH41 1LD, UK

<sup>2</sup>Institute for Astronomy, University of Hawaii, 2680 Woodlawn Drive, Honolulu, HI 96822

<sup>3</sup>Astrophysics Group, Blackett Laboratory, Imperial College, Prince Consort Road, London, SW7 2AZ, UK

<sup>4</sup>Institute for Astronomy, University of Edinburgh, Royal Observatory, Blackford Hill, Edinburgh, EH9 3NJ, UK

<sup>5</sup>Visiting Astronomer at the NASA Infrared Telescope Facility, which is operated by the University of Hawaii under contract from the National Aeronautics and Space Administration.

mology with  $H_0 = 50 \text{ km s}^{-1} \text{ Mpc}^{-1}$  is assumed, and X-ray luminosities ( $L_x$ ) are quoted for the 0.3–3.5 keV pass band.

## 2. DATA

### 2.1. Sample

The data presented here comprise K-band observations of 76 BCGs. This sample, which incorporates that of CM98, spans a redshift range of 0.05 to 0.83, and is drawn from the following X-ray selected cluster catalogues: the Einstein EMSS (Gioia & Luppino 1994; Nichol et al. 1997; Henry 1999), the Southern and Bright SHARC catalogues (Burke et al. 1997; Romer et al. 2000), and the ROSAT NEP Survey (Henry et al. 1997). X-ray selection is to be preferred, since both X-ray luminosity and X-ray temperature should be more closely related to cluster mass than optical richness.

The X-ray luminosity-redshift coverage of the cluster sample is shown by the circles in Figure 1. The additional symbols show those clusters from ABK98 with a measured X-ray flux or upper limit, except for Cl 2155+0334 (also known as Cl 2157+0347), which has been removed because photometric and spectroscopic observations show no evidence for a cluster (Thimm & Belloni 1994; Oke, Postman & Lubin 1998), and Cl 0016+16, since it is in both samples. The difference in X-ray luminosity coverage at  $z > 0.5$  for the two samples is striking; the implications of this are discussed in section 3.

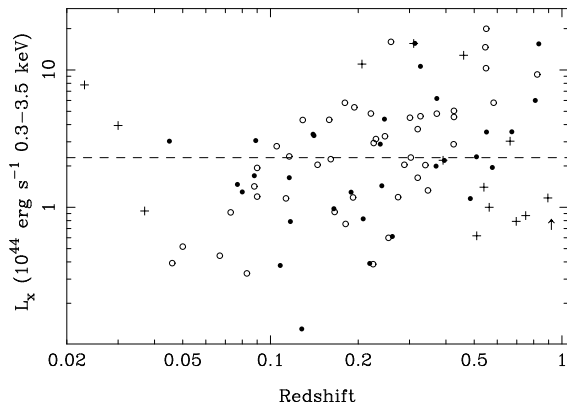


FIG. 1.—Cluster X-ray luminosity as a function of redshift. The circles indicate the BCG sample presented here; open for clusters used in CM98 and filled for the new observations. Clusters from ABK98 with measured X-ray fluxes are shown as plus (+) symbols and the arrow ( $\uparrow$ ) symbol represents the  $3\sigma$  upper limit for Cl 1603+4329. The dashed line, at  $L_x = 2.3 \times 10^{44} \text{ erg s}^{-1}$ , shows the luminosity used by CM98 to separate their sample into high- and low- $L_x$  clusters.

The K-band BCG observations were made using the IRCAM3 and UFTI cameras on the UKIRT and NSFCAM on the IRTF, with some of the data being provided by the service programs of both telescopes. IRCAM3 and NSFCAM are 256x256 pixel InSb devices with a field of view close to  $70''$  by  $70''$  (the IRCAM3 and NSFCAM pixel scales are  $0.281$  and  $0.3'' \text{ pixel}^{-1}$  respectively), and UFTI is a  $1024 \times 1024$  pixel HgCdTe array with a pixel scale of  $0.091'' \text{ pixel}^{-1}$ , giving a field of view of  $92''$  by  $92''$ . The observing strategy is the same as presented in CM98: the BCGs were imaged using a jitter pattern and separate sky

exposures were taken for those objects which filled the field of view.

### 2.2. Reduction

The data reduction system improves upon that presented in CM98, and incorporates elements from the methods described in Stanford, Eisenhardt & Dickinson (1995) and Hall, Green & Owen (1998). An outline is presented below as the method will be fully described in a later paper.

The individual frames were masked for bad pixels, dark subtracted and divided by the exposure time. A flat field image was created by median combination of the object images—or separate sky exposures if these were available—and applied to the object frames. Masking of cosmic ray events was performed on the flattened images before they were mosaiced together, which completed the processing of those objects with sky exposures. Otherwise the mosaic—which is substantially deeper than the individual exposures—was used to create an object mask, which was then applied to the individual images before they were median-combined to form a flat. The flattened exposures were then processed as above to create the final image.

Observations of stars from the UKIRT faint standards list (Casali & Hawarden 1992) were used to calibrate the photometry onto the UKIRT system assuming an extinction of  $0.088 \text{ mag airmass}^{-1}$ , the median value for K-band observations at Mauna Kea. Comparisons of the results from repeat observations, both within and between observing runs, show that the magnitudes agree to  $0.05 \text{ mag}$ .

Aperture magnitudes were measured using a  $50 \text{ kpc}$  diameter aperture and have been corrected for Galactic absorption using the maps of Schlegel, Finkbeiner, & Davis (1998): the correction is small, mostly being less than  $0.05 \text{ mag}$ , but reaching  $0.1 \text{ mag}$  in several cases. The position of the aperture was chosen so as to maximise the flux contained within it whilst remaining close to the center of the cluster X-ray emission. Those pixels contaminated by stars and obvious non-cluster galaxies were excluded from the calculation, being replaced by values chosen from regions at the same distance from the aperture center. No attempt has been made to remove flux due to other cluster galaxies falling within the aperture, and so the results are directly comparable to those of ABK98.

## 3. RESULTS

The K-band Hubble diagram for the two BCG samples is shown in Figure 2. The lines show model predictions calculated using the GISEL96 code (Bruzual & Charlot 1993), for a solar-metallicity stellar population with a Salpeter initial mass function: the solid line indicates a no-evolution model for a  $10 \text{ Gyr}$  old stellar population, whereas the other lines are for stellar populations which form in an instantaneous burst of star formation at a single epoch— $z_f = 2$  for the dashed line and  $z_f = 5$  for the dotted line—and then evolve passively. The models have been normalised to match the low-redshift, X-ray selected, BCG sample of Lynam et al. (1999), following the method used in ABK98, assuming a growth curve,  $d \log L / d \log r$ , of  $0.7$  for the aperture corrections and a color of  $R - K = 2.6$ .

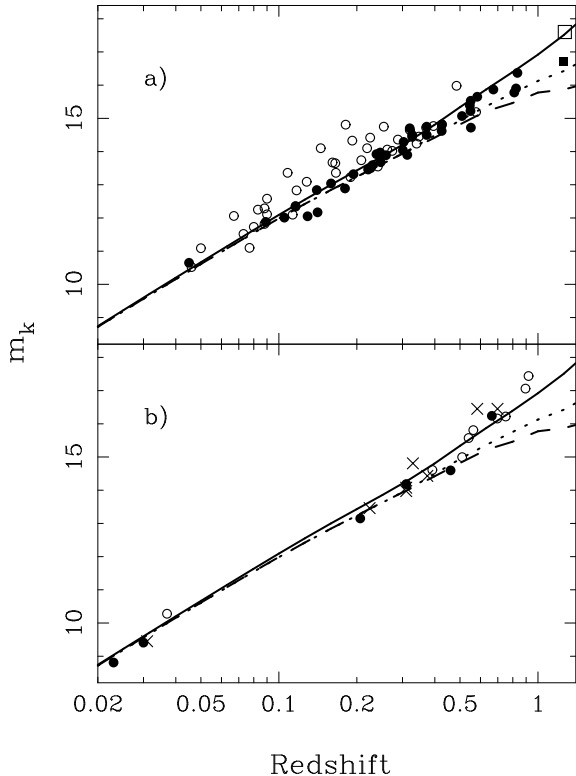


FIG. 2.—Magnitude-redshift relation for brightest cluster galaxies in the observed K band. Filled and open symbols represent those BCGs in high- and low- $L_x$  clusters respectively; the division is as in Figure 1. The circles in the top panel indicate the sample presented here, whilst the squares are for the BCGs in the two  $z = 1.3$  clusters from Rosati et al. (1999), where the magnitudes have been measured within 50 kpc diameter apertures (P. Rosati 1999, private communication). The bottom panel shows the sample of ABK98, where the crosses are for those clusters without a measured X-ray flux. The no-evolution prediction, assuming a 10 Gyr old stellar population, is shown by the solid line; passive-evolution models, in which the stars form at a single epoch, are shown as dashed ( $z_f = 2$ ) and dotted ( $z_f = 5$ ) lines.

The result remains qualitatively the same as Figure 6 of CM98; BCGs in high- $L_x$  clusters form a homogeneous population which is brighter, and has a smaller scatter, than that of low- $L_x$  clusters. This can be more clearly seen in Figure 3, which shows the scatter around the model predictions as a function of cluster X-ray luminosity. It is this relationship between BCG and cluster properties that leads to the contradictory conclusions of CM98 and ABK98: out of the eleven  $z > 0.5$  clusters in the latter sample, nine have X-ray flux measurements or upper limits, with all but two of these having a low X-ray luminosity (Figure 1). It is unsurprising that these clusters are not similar to rich, local clusters, as they were discovered on the basis of their optical properties (e.g. Castander et al. 1994; Holden et al. 1997). The squares in Figure 2 represent the BCGs in the two  $z = 1.3$  clusters discussed by Rosati et al. (1999): the high- $L_x$  cluster (solid square) was discovered by means of its X-ray emission, whereas the low- $L_x$  cluster (open square) was detected by its galaxy population. Although based on only two points, this sug-

gests that the correlation with environment holds at this redshift.

The semi-analytic models discussed in ABK98 predict a factor of  $\sim 4$ –5 increase in the stellar masses of BCGs in massive clusters since  $z = 1$ , for an Einstein-de Sitter universe. To test whether the data presented here supports this level of evolution, a correlation between redshift and the BCG residuals ( $\Delta m_k$ , e.g. Figure 4) has been sought. Passive-evolution models with  $z_f = 2$  and  $z_f = 5$  have been used to calculate the residuals—since they provide a conservative range for the formation epoch of massive cluster ellipticals (e.g. Ellis et al. 1997)—and separate fits made to the high- and low- $L_x$  cluster subsamples. Since the form of any evolution is unknown a priori, a non-parametric rank-order statistic—Kendall’s  $\tau$ —was used; it also has the advantage that it is insensitive to the choice of normalisation adopted for the Bruzual & Charlot models. All save one of the fits showed no significant ( $> 3\sigma$ ) evidence for evolution; the exception, at a significance of  $3.6\sigma$ , was the high- $L_x$  subsample with  $z_f = 2$ . To find the maximum formation epoch that is still compatible with evolution of the high- $L_x$  subsample,  $z_f$  was increased from 2 until the correlation significance dropped below  $3\sigma$ . Evolution is found only if the stars formed recently ( $z_f \leq 2.6$ ).

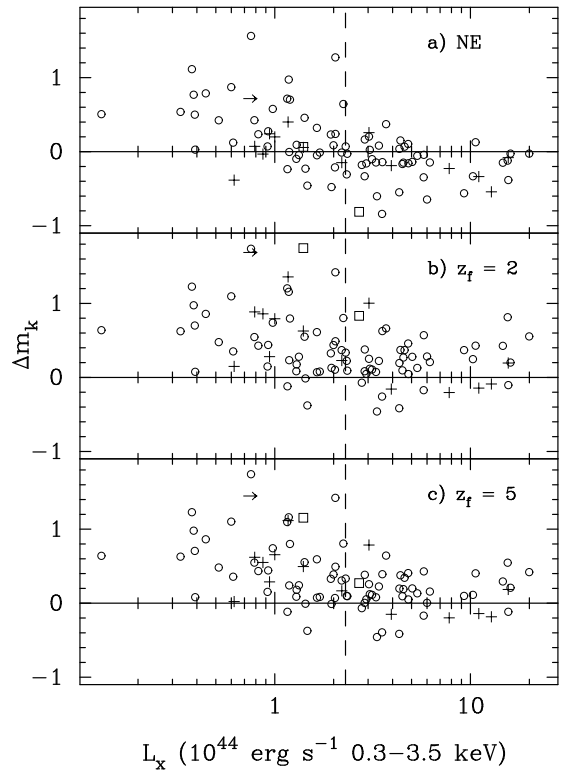


FIG. 3.—Residuals about the model predictions, defined as  $\Delta m_k = m_{\text{BCG}} - m_{\text{model}}$ , as a function of cluster X-ray luminosity. The BCGs presented here are shown as circles, the sample of ABK98 is shown as in Figure 1, and the squares represent the two clusters from Rosati et al. (1999). The three panels are for the models shown in Figure 2: a) no-evolution model for a 10 Gyr old stellar population, b) formation at a redshift of 2 followed by passive evolution, and c) as for b) but with a formation redshift of 5.

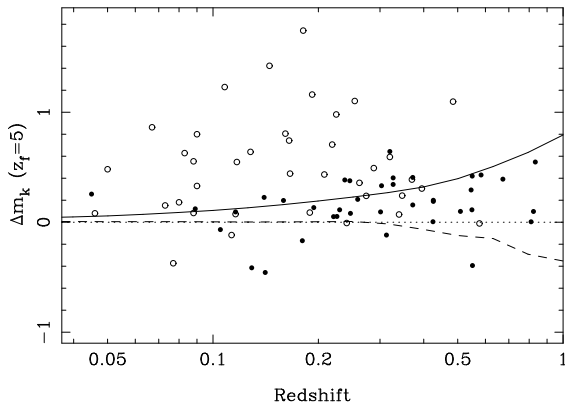


FIG. 4.—Residuals about the  $z_f = 5$  model for the X-ray selected BCG sample. Filled and open symbols indicate BCGs in high- and low- $L_x$  clusters respectively. The lines show the expected locus of the residuals for the three models shown in Figure 2.

To quantify the amount of evolution allowed by the data, the same parametric form as employed by ABK98—namely  $M(z) = M(0) \times (1+z)^\gamma$ —was used to estimate the growth in the stellar mass content of BCGs. Fitting for both  $\gamma$  and  $M(0)$  indicates that, in the high- $L_x$  sample (which best approximates the cluster selection adopted for the semi-analytic models), the typical BCG mass has increased by a factor of  $1.9 \pm 0.3$  (for  $z_f = 2$ ) or  $1.3 \pm 0.2$  ( $z_f = 5$ ) between  $z = 1$  and the present. These growth factors are substantially lower than either the factor of  $\sim 4$ –5 predicted by the semi-analytic models, or the measured values of 4.6 ( $z_f = 2$ ) and 3.2 ( $z_f = 5$ ), of ABK98. The growth factor can also be estimated by fitting for  $\gamma$  alone if one assumes a low-redshift normalisation for the model predictions. However, this currently involves applying a color-correction to low-redshift optical BCG data, which introduces further uncertainty: applying a single  $R - K$  correction to the X-ray-selected sample of Lynam et al. (1999) changes the measured growth factor of the high- $L_x$  sample by less than 20%, whilst using the normal-

isation adopted by ABK98—based on an optically-selected sample—increases the growth factor by 50%. K-band observations of the Lynam et al. (1999) sample are being obtained to circumvent this problem in future work.

#### 4. CONCLUSION

The K-band luminosities of BCGs are correlated with their environment: clusters with a high X-ray luminosity contain BCGs which are brighter, and have a smaller scatter, than those BCGs in clusters with a low X-ray luminosity. The BCG evolution seen by ABK98 has been shown to be an artifact of a selection bias in their cluster sample; at high redshifts, their clusters are systematically less X-ray luminous than their low-redshift sample, and so their BCGs are systematically fainter.

Under the assumption of an Einstein-de Sitter universe, non-parametric tests show that the only significant evidence for BCG mass evolution over the range  $0.05 \leq z \leq 0.83$  occurs when the dominant stellar population formed relatively recently ( $z_f \leq 2.6$ ). Using the same parametric form as ABK98, the masses of BCGs in high- $L_x$  clusters are found to have, at most, doubled since  $z = 1$ , compared to the factor of  $\sim 4$  increase predicted, for BCGs in massive clusters, by the semi-analytic models discussed by ABK98.

DJB acknowledges support from PPARC grant GR/L21402 and SAO contract SV4-64008 and RGM that from PPARC at Imperial College and Edinburgh. DJB would like to thank Peter Draper, Tim Hawarden, and Sandy Leggett for useful discussions. We thank the referee, Alfonso Aragón-Salamanca, for useful comments that improved the paper, the service programs of both UKIRT and IRTF for obtaining some of the data presented here, and Piero Rosati and collaborators for providing aperture magnitudes for the two Lynx clusters. The United Kingdom Infrared Telescope is operated by the Joint Astronomy Centre on behalf of the U.K. Particle Physics and Astronomy Research Council.

#### REFERENCES

- Aragón-Salamanca, A., Baugh, C. M., & Kauffmann, G. 1998, MNRAS, 297, 427 (ABK98)
- Aragón-Salamanca, A., Ellis, R. S., Couch, W. J., Carter, D. 1993, MNRAS, 262, 764
- Baugh, C. M., Cole, S., & Frenk, C. S. 1996, MNRAS, 282, L27
- Bershady, M. A. 1995, AJ, 109, 87
- Bruzual A., G. & Charlot, S. 1993, ApJ, 405, 538
- Burke, D. J., Collins, C. A., Sharples, R. M., Romer, A. K., Holden, B. P., & Nichol, R. C. 1997, ApJ, 488, L83
- Collins, C. A., & Mann, R. G. 1998, MNRAS, 297, 128 (CM98)
- Casali, M. M., & Hawarden, T. G. 1992, The JCMT-UKIRT Newsletter, No. 3, 33
- Castander, F. J., Ellis, R. S., Frenk, C. S., Dressler, A., & Gunn, J. E. 1994, ApJ, 424, L79
- De Propris, R., Stanford, S. A., Eisenhardt, P. R., Dickinson, M., & Elston, R. 1999, AJ, 118, 719
- Dressler, A. 1978, ApJ, 222, 23
- Eggen, O. J., Lynden-Bell, D., & Sandage, A. R. 1962, ApJ, 136, 748
- Ellis, R. S., Smail, I., Dressler, A., Couch, W. J., Oemler, A., Butcher, H., & Sharples, R. M. 1997, ApJ, 483, 582
- Gioia, I. M., & Luppino, G. A. 1994, ApJS, 94, 583
- Hall, P. B., Green, R. F., & Cohen, M. 1998, ApJS, 119, 1
- Henry, J. P., et al. 1997, AJ, 114, 1293
- Henry, J. P. 1999, ApJ, submitted
- Holden, B. P., Romer, A. K., Nichol, R. C., & Ulmer, M. P. 1997, AJ, 114, 1701
- Jimenez, R., Friaca, A., Dunlop, J., Terlevich, R., Peacock, J., & Nolan, L. 1999, MNRAS, 305, L16
- Kauffmann, G., & Charlot, S. 1998, MNRAS, 294, 705
- Kauffmann, G., & White, S. D. M. 1993, MNRAS, 264, 201
- Larson, R. B. 1969, MNRAS, 145, 405
- Lynam, P. D., Collins, C. A., James, P. A., Böhringer, H., & Neumann, D. M. 1999, preprint (astro-ph/9908348)
- Madau, P., Pozzetti, L., & Dickinson, M. E. 1998, ApJ, 498, 106
- Nichol, R. C., Holden, B. P., Romer, A. K., Ulmer, M. P., Burke, D. J., & Collins, C. A. 1997, ApJ, 481, 644
- Oke, J. B., Postman, M., & Lubin, L. M. 1998, AJ, 116, 549
- Poggianti, B. M., Smail, I., Dressler, A., Couch, W. J., Barger, A. J., Butcher, H., Ellis, R. S., & Oemler, A., Jr. 1999, ApJ, 518, 576
- Romer, A. K., et al. 2000, ApJS, in print
- Rosati, P., Stanford, S. A., Eisenhardt, P. R., Elston, R., Spinrad, H., Stern, D., & Dey, A. 1999, AJ, 118, 76
- Schlegel, D., Finkbeiner, D., & Davis, M. 1998, ApJ, 500, 525
- Stanford, S. A., Eisenhardt, P. R., & Dickinson, M. 1995, ApJ, 450, 512
- Stanford, S. A., Eisenhardt, P. R., & Dickinson, M. 1998, ApJ, 492, 461
- Thimm, G. J., & Belloni, P. 1994, A&A, 289, L27
- van Dokkum, P. G., & Franx, M., 1996, MNRAS, 281, 985
- van Dokkum, P. G., Franx, M., Kelson, D. D., & Illingworth, G. D. 1998, ApJ, 504, L17
- van Dokkum, P. G., Franx, M., Fabricant, D., Kelson, D. D., & Illingworth, G. D. 1999, ApJ, 520, L95